Title

Experimental analysis of a low cost phase change material emulsion for its use as thermal storage system

Authors

Mónica Delgado*, Ana Lázaro, Javier Mazo, Conchita Peñalosa, Pablo Dolado, Belén Zalba

Aragón Institute for Engineering Research (I3A), Thermal Engineering and Energy Systems Group, University of Zaragoza
Agustín Betancourt Building, C/María de Luna 3, 50018 Zaragoza, Spain
Phone: (+34) 876 555 584

* Corresponding Author, monica@unizar.es

Email addresses: ana.lazaro@unizar.es (Ana Lázaro), jmazo@unizar.es (Javier Mazo), conchita.penalosa@unizar.es (Conchita Peñalosa), dolado@unizar.es (Pablo Dolado), bzalba@unizar.es (Belén Zalba)

Abstract

A 46 liter commercial tank with a helical coil heat exchanger and containing a low cost phase change material emulsion has been experimentally analyzed as a thermal energy storage system in terms of volumetric energy density and heat transfer rate, for its subsequent comparison with other thermal energy storage systems. This phase change material emulsion shows a phase change temperature range between 30-50ºC, its solids content is about 60% with an average particle size of 1 μm. The low cost phase change material emulsion shows a thermal storage capacity by mass 50% higher than water and an increase in viscosity up to 2-5 orders of magnitude. The results have shown that the global heat transfer coefficient of the phase change material emulsion tank is around 2-6 times higher than for conventional latent systems previously analyzed in literature, although 5 times lower than if it contains water. The phase change material emulsion tank presents an energy density 34% higher than the water tank, which makes it a promising solution. Measures to improve its performance are also studied in this work.

Keywords: Phase change material slurry, Phase change material emulsion, PCM, Natural convection heat transfer, Thermal energy storage density

Nomenclature

A	Heat transfer area (m^2)	E	Energy (J)
c_p	Specific heat (J/(kg·K))	F	Correction factor for the average temperature difference in heat exchangers (-)
D_H	Helical coil diameter (m)		
d	Tube diameter (m)		

h Convective coefficient (W/(m^2·K))

$\dot{m}$ Mass flow (kg/s)

m Mass (kg)

$\dot{Q}$ Heat (W)

T Temperature (ºC)

t Time (s)

U Global heat transfer coefficient (W/(m^2·K))

V Volume (m^3)

ΔT Temperature difference (ºC)

Greek symbols

λ Thermal conductivity (W/(m·K))

Abbreviation

COP Coefficient of Performance

DSC Differential Scanning Calorimetry

HTF Heat Transfer Fluid

PCM Phase Change Material

TES Thermal Energy Storage

1D One-dimension

2D Two-dimensions

Dimensionless numbers

Bi Biot number (-)

De Dean number (-)

Nu Nusselt number (-)

Pr Prandlt number (-)

Ra Rayleigh number (-)

Re Reynolds number (-)

Subscripts

amb Ambient

e End

ext External

i Initial

in Inlet

Int Internal

m	Mean, average	out	Outlet
ml	Mean logarithmic	w	Water

1. Introduction

Generally called PCM slurries consist of biphasic fluids from the mixture of a fluid such as water and a phase change material (PCM). PCM slurries are being widely studied because of their potential contribution for a sustainable energy model. Research efforts over the last 10 years have resulted in considerable progress in the study of these new latent fluids. The interest in these new fluids can be demonstrated with the recent publication of four comprehensive reviews: the review of Chen et al. [1], which deals with the thermal and hydrodynamic properties of microencapsulated PCM slurries; the overview of Zhang et al. [2], which also investigates semi-clathrate hydrate slurries; the review of Delgado et al. [3], which is completed by the analysis of PCM emulsions; and the state of the art of Youssef et al. [4], gathering additional information about shape-stabilized PCM slurries. This interest is also proved with the development of such fluids by several companies and research institutes such as BASF [5], AERO [6], Fraunhofer ISE [7] and Fraunhofer UMSICHT [8], among others. These new fluids offer many advantages and can be used either as TES or as a heat transfer fluid (HTF) due to their following features [9]: 1) high storage capacity during phase change in comparison to water; 2) the possibility of using the same medium either to transport or to store energy, as these dispersions are pumpable, thus reducing heat transfer losses; 3) heat transfer at an approximately constant temperature; 4) high heat transfer rate due to the high surface/volume ratio; 5) lower pumping requirements, as a consequence of the reduction in mass flow due to higher heat capacity.

Although PCM slurries have numerous advantages, there is still a lack of experience concerning their technical feasibility. The main challenge in their use as thermal storage material is the heat transfer during the charge and discharge processes in comparison to traditional storage systems, such as water tanks using sensible heat storage, and in comparison to storage systems where the PCM is macroencapsulated in different geometries or is directly confined in the tank. Several researchers have experimentally studied tanks with typical spiral type internal heat exchangers, flowing water through the coil as a HTF and containing PCM slurries as thermal storage material. Heinz and Streicher [10] studied a 200 liter tank with a microencapsulated PCM slurry developed by BASF, with a melting temperature of 60ºC. As the limiting factor for the heat transfer is the natural convection from the exchanger surface to the storage fluid, it was interesting to analyze the natural convective heat transfer coefficient. Due to the higher viscosities, this coefficient decreased when increasing the PCM concentration in water. Even with the lowest PCM concentration, 20%, these heat transfer coefficients were lower than for water. A very similar study was carried out by Diaconu et al. [11] who studied heat transfer by natural convection in a tank filled with a microencapsulated RT6 slurry. During the phase change, the natural convective coefficient could be up to five times higher than for water, depending on the temperature conditions. The authors could not provide the reasons for this improvement, since the phase change temperature range overlapped with the temperature range in which the water showed a drop in the natural convection. Huang et al. [12] also studied a TES system with a helical coil as heat exchanger, using a microencapsulated PCM slurry with a phase change temperature of 65ºC (produced by BASF) with a PCM volumetric concentration of 25, 35 and 50%. The results showed that the PCM slurry with a 50% concentration was not appropriate, since the low thermal conductivity and the high

viscosity reduced the heat transfer from the exchanger to the storage medium. None of these works has shown the complete characterization of PCM slurries properties for a better understanding of the results Furthermore, authors have not compared the results obtained with other latent TES systems to analyze the improvement level that these new TES systems could have.

In view of these previous researches, the objective of the current work is the experimental study of an inexpensive TES system with an increased volumetric energy density in comparison to water, and an improved charge/discharge rate in comparison to traditional TES systems with PCM. To date, attempts to solve the low charge /discharge rate of traditional TES systems with PCM have focused on increasing the heat transfer surface or enhancing the PCM thermal conductivity [13], which leads to more expensive systems. In this case, a commercial tank containing a low cost PCM emulsion as heat storage material has been analyzed and compared to other TES systems in terms of volumetric energy density and heat transfer rate. Their thermophysical and rheological properties have been determined for a better understanding of the experimental results in terms of TES capacity and heat exchange. In addition, the complete characterization of the material is a valuable information for further developments of the TES system.

2. Materials and properties

Researchers are starting to look for by-products and waste-products to be used as PCM, in order to reduce the price and the environmental cost associated with their TES systems. The energy saving potential of PCMs has been proven, but high PCM prices have hindered their extension. As Kosny et al. [14] explained in their study, PCM prices are driven by market

demand and supply relationships. For the moment, the PCM market is not yet fully developed, resulting in limited demand that is largely responsible for the relatively higher prices. As example, Peñalosa et al. [15] apply a methodology to look for low cost PCMs from waste products, byproducts or natural products and Biswas and Abhari [16] use in their research a low cost bio-PCM in building envelope applications. In addition to the PCM price, the cost of encapsulation must also be considered, which sometimes represents an important percentage of the final PCM product, as Dolado's study [17] shows. In his final PCM product, the cost of the PCM in the CSM Panels containing RT27 developed by Rubitherm represented only 18-23% of the total cost.

In this research, a PCM emulsion has been analyzed in which the emulsified PCM is a low cost paraffin, specifically a by-product of the petroleum refining process. This PCM emulsion is in turn a co-product, since to date it has been used for other purposes unrelated to the purpose presented here. Given that it is an emulsion, the extra cost of the microencapsulation process is avoided. Nevertheless instabilities processes such as coalescence may occur more easily [18]. According to the technical specifications supplied by the manufacturer, the solids content of this PCM emulsion is about 59-61%, with an average particle size of 1 μm.

2.1 Thermophysical characterization

2.1.1 Enthalpy-temperature curves

The enthalpy-temperature curve of the PCM emulsion has been obtained in order to know the storage capacity in the phase change temperature range of the paraffin in emulsion. Due to the phase change temperature of the sample and the temperature limitations of the

89 current installation in our laboratory (5-40ºC) [19] based in the T-history methodology
90 proposed by Zhang et al. [20]. This setup has been used only for the cooling tests. The
91 heating tests have been executed with a DSC. The cooling tests could also have been
92 executed with the DSC; however, the DSC cooling system with liquid nitrogen does not
93 allow good control when working with low cooling rates.

94 The volume of the sample should be at least a few cm^3 or more if possible to ensure that it
95 has the correct chemical and physical composition representative of the bulk material, 10
96 cm^3 in the current T-history installation. The verification of the installation of the T-history
97 method was accomplished through the calibration of the sensors, the verification of the
98 measurement of temperature and the verification of the measurement of the enthalpy
99 variation [21]. Two pure substances were employed with a constant phase change
100 temperature and known phase change enthalpy (gallium and hexadecane). In the
101 determination of the enthalpy, the difference was lower than 12% in all cases.

102 As previously mentioned, the melting curve was obtained with a DSC 200 F3 Maia
103 manufactured by Netzsch. The tests were executed at a heating rate of 0.5 K/min with a
104 sample mass of about 10 milligrams. This heating rate was chosen from previous thermal
105 equilibrium tests according to a standardized measurement procedure defined by several
106 round robin tests [22]. Following this standard, a deviation lower than 5% can be associated
107 to the error in the enthalpy measurements [23].

108 Figure 1 shows the melting and solidification curves obtained compared to the water curve.
109 An increase of 50% in the energy storage capacity per mass is observed in the temperature
110 range of 30-55ºC. It must be pointed out that the phase change temperature range is quite

111 wide, since the sample is a by-product and purification processes have not been carried out.
112 Hysteresis is also observed between the melting and solidification curves.

113 2.1.2 Thermal diffusivity-temperature curves

114 The thermal diffusivity-temperature curves of the PCM emulsion were determined using a
115 Laser Flash device; an LFA 457 Microflash manufactured by Netzsch. The Laser Flash
116 method was initially designed for measurements in solids where the thickness is known. To
117 measure the thermal diffusivity in liquids, a special sample holder is necessary to contain
118 the PCM emulsion. For these measurements a Pt90Rh10 sample holder supplied by
119 Netzsch was used. The considerations proposed by the authors in a previous article were
120 taken into account when doing the measuring [24]. To determine the accuracy of the
121 measurements, three liquids whose thermal diffusivity value is known were measured:
122 distilled water, hexadecane and glycerin. An error range of 4.31-15.38% was achieved.

123 Figure 2 shows the results obtained for three different samples of the PCM emulsion
124 analyzed. The values represented are the average value of five repetitions at each set
125 temperature, together with the standard deviation. The thermal diffusivity values obtained
126 in comparison to those of water decreased significantly, by about 40%. The thermal
127 conductivity value for the PCM emulsion at 50ºC, calculated from the heat capacity,
128 thermal diffusivity and density values (this last property determined in the following
129 subsection 2.1.3) was 0.27 W/(m·K), as against 0.63 for water. Measurements executed in
130 previous studies on other commercial PCM slurries did not show such low thermal
131 conductivity values, even though it is true that the PCM concentration in suspension was
132 lower [24].

2.1.3 Density-temperature curves

To complete the thermophysical characterization of the PCM emulsion, the density was measured with a model DM-40 densimeter supplied by Mettler-Toledo, which uses the oscillating U-tube method. This property is necessary in order to know the expansion experienced by the PCM emulsion during heating and also to know the storage energy density. The instrument constants of the densimeter oscillator were obtained through the adjustment with air and distilled water, whose density values are known. After this adjustment process, accomplished at different temperature levels, distilled water and liquid octadecane at 60ºC were measured as reference materials, observing a deviation in density lower than 0.1%.

Figure 3 shows the values obtained for three different temperature levels: 20, 40 and 60ºC. The values represented are the average density values of three different samples, together with the standard deviation in density. It is observed that the density variation with temperature is higher than for water, that is to say the volumetric expansion coefficient of the PCM emulsion is higher, boosting in this manner the buoyancy forces and therefore the convection phenomenon during the heat transfer in tanks with this substance.

2.2 Rheological characterization

The viscosity-shear rate and viscosity-temperature curves were obtained with a control stress rheometer supplied by TA instruments, model AR-G2. This viscosity has an influence on the heat transfer process, and it is necessary when calculating the pumping requirements in the use of the PCM emulsion as HTF.

154 The procedure proposed by Delgado et al. [25] for the viscosity measurement of PCM
155 slurries was followed. A plate geometry with a diameter of 40 mm was used. The sample
156 was covered during the tests with a solvent trap to avoid its evaporation. The tests were
157 performed at 25ºC. A Peltier plate was used as a temperature controller.

158 Figure 4 shows the results. It is observed that the PCM emulsion shows a pseudoplastic
159 behavior and that its viscosity is significantly higher than that of water, especially when
160 values at low shear rates are compared. The viscosity is up to five orders of magnitude
161 larger in this range. This low shear rate would correspond with the PCM emulsion at rest
162 situation, when it is contained in the tank. Such high viscosity will cause the viscous forces
163 to prevail over the buoyancy forces, therefore not boosting the convection phenomenon.
164 Other PCM slurries analyzed to date have shown a lower viscosity, about one order of
165 magnitude lower [24], but they also had a lower paraffin concentration in suspension.
166 Figure 5 shows the variation of the viscosity with temperature. It is observed that the
167 viscosity increases significantly from 45ºC. It is also observed that after the first melting,
168 the sample viscosity at room temperature increased due to a degradation process of the
169 sample, according to the manufacturer's information. This increase was observed only after
170 the first melting. No significant changes in the rest of the properties were observed after
171 this degradation.

172 To assess the deviation of the viscosity values obtained, viscosity measurements of a
173 standard oil S60 supplied by Paragon Scientific were carried out under similar conditions of
174 temperature and of torque (from 0.02 to 1200 μN·m). An average deviation of 5.5% at 25ºC
175 and 11.7% at 50ºC was obtained.

3. Heat transfer study of the paraffinic emulsion contained in a tank for use as thermal storage material

3.1 Description of the experimental installation

A storage tank supplied by the Spanish manufacturer Lapesa was tested for analysis of the natural convection in these new thermal storage fluids. Generally these types of tank are manufactured with carbon steel, namely with the S275JR alloy, to keep the price as low as possible. However, since the paraffinic emulsion contains water, and this plays an important role in metal corrosion, the tank selected was made of stainless steel AISI 316 to avoid possible corrosion phenomena. Corrosion products could cause destabilization in the PCM emulsion, and therefore hinder the present study. In parallel, corrosion tests were carried out in accordance with the standard G1 of the American Society for Testing and Materials [26]. No significant corrosion rates were observed. Corrosion was lower for the emulsion than for water.

The tank volume is 46 liters, its internal diameter 29.5 cm and its length 83.5 cm. It has an internal coil working as a heat exchanger. The internal diameter of this coil is 23 mm and its wall thickness 1 mm. Its heat exchange surface is 0.71 m^2. The tank was isolated with polyurethane with a thickness of 4.25 cm.

The HTF is water, which enters the coil through the lower part and leaves through the upper part. Two 4 wire-Pt100 sensors were used to measure the water temperature at the inlet and outlet of the coil. These resistance temperature sensors are mineral insulated, 1/3 DIN, with a stainless steel sheath with a diameter of 3 mm and a length of 180 mm. The sensors were introduced in parallel to the tube through an adjustable compression fitting.

198 Both temperature sensors were calibrated at three temperature levels: 25, 50 and 75ºC. The
199 maximum deviation observed in these sensors according to the calibration report is 0.04ºC.

200 For the temperature measurement in the thermal storage fluid, 7 Pt100 sensors were placed
201 along the central axis of the tank, separated by a distance of 10.5 cm. Their technical
202 specifications are the same as those used for the temperature measurement of the HTF. The
203 temperature sensors were all calibrated at three temperature levels: 25, 50 and 75ºC,
204 observing in this case a maximum deviation of 0.15ºC. The sensors were placed in the tank
205 using a multiple sensor feed through sealing assembly. Each of these sensors was
206 introduced a certain length so that they were separated equidistantly along the central axis.
207 For the seven measurement points, the immersion depth was higher than the minimum
208 immersion depth required by the calibration tests. Figure 6 shows the tank and the point
209 where the temperature sensors were placed along the central axis of the tank.

210 The flow mass measurement of the HTF was made with a Coriolis mass flow meter, which
211 has an accuracy of 0.1% for liquids. The establishment of the initial conditions of the tank,
212 as well as the flow temperature of the HTF, was controlled by a thermostatic bath, a Hüber
213 model Unichiller UC040T. Its temperature stability is 0.1 K. Further technical details of the
214 installation to which the tank was connected can be found in a previous article by Delgado
215 et al. [27].

216 **3.2 Tests using water as thermal storage material**

217 Heating tests were performed using water as both HTF and TES material. The temperature
218 levels were selected according to the phase change temperatures of the PCM emulsion to be
219 analyzed. The initial temperature of the stored water was 30ºC and the flow temperature of

220 the water as HTF was 50, 55 and 60ºC. The mass flow was selected according to the
221 pumping limitations of the thermostatic bath: 150, 270 and 420 kg/h.

222 Figure 7 shows the temperature evolution of the water stored in the tank. The temperature
223 increases, and no significant temperature differences between the measurements of the
224 sensors from position 1 to position 6 are observed. The heating rate of the water in the
225 lower part of the tank, recorded by the sensor in position 7, is lower. This is due to the fact
226 that the water volume corresponding to the measurement of this probe is located below the
227 coil. Figure 6 shows how the coil does not occupy the lower section recorded by sensor 7.
228 The heat transfer towards this section is predominantly by conduction and not by
229 convection, giving rise to a dead volume whose dynamic is slower.

230 **3.2.1 Obtaining the global heat transfer coefficient**

231 If the energy balance on the coil (equation 1) is carried out from the measurements obtained
232 during the transient response, the global heat transfer coefficient can be obtained:

233 $$\dot{m} \cdot c_p \cdot (T_{in} - T_{out}) = U \cdot A \cdot \Delta T_m \quad \text{(eq. 1)}$$

234 The temperature difference between the fluid flowing through the coil and the fluid stored
235 in the tank changes along the heat exchanger, so it is advisable to estimate a mean
236 temperature difference, ΔT_m. This mean temperature difference for every instant can be
237 calculated as the logarithmic mean temperature difference, according to equations 2, 3 and
238 4:

239 $$\Delta T_{ml} = \frac{\Delta T_{position\ 6} - \Delta T_{position\ 2}}{ln\left(\frac{\Delta T_{position\ 6}}{\Delta T_{position\ 2}}\right)} \quad \text{(eq. 2)}$$

$$\Delta T_{position\ \ 6} = T_{in} - T_{water\ tank\ 6} \quad \text{(eq. 3)}$$

$$\Delta T_{position\ \ 2} = T_{out} - T_{water\ tank\ 2} \quad \text{(eq. 4)}$$

It is also advisable to relate the equivalent temperature difference with the relation of the logarithmic mean difference by means of a correction factor F. In the case that in one of the sides of the heat exchanger there is phase change, this correction factor F can be considered 1. In the present case, it can be observed that there is no significant temperature gradient with position in the external side of the coil. Therefore a factor F=1 has been adopted.

Figure 8 shows the global heat transfer coefficient obtained at every instant during the transient response of the different tests and its dependence on the average temperature difference and on the temperature difference of the HTF. Figure 9 shows this global heat transfer coefficient for some of the tests, together with the deviations calculated from the error propagation formula. In these calculations the error of each variable has been considered according to the deviations observed in the calibration processes. The highest contribution to the deviation is caused by the uncertainty of the average temperature difference. For this reason the deviation is higher at low values of this average temperature difference.

Once the global heat transfer coefficient U has been determined by means of an analysis of the thermal resistances, and by calculating from correlations the interior forced heat transfer coefficient in the helical coil, the natural convective heat transfer coefficient in the stored water, external to the coil, can be obtained. Equation 5 shows the equation from the analysis of thermal resistances:

$$\frac{1}{U_{ext}} = \frac{1}{h_{ext}} + \frac{d_{ext}}{2\cdot\lambda}\cdot ln\left(\frac{d_{ext}}{d_{int}}\right) + \frac{d_{ext}}{d_{int}}\cdot\frac{1}{h_{int}} \quad \text{(eq. 5)}$$

To calculate the convective heat transfer coefficient in the inner part of the helical coil h_{int}, firstly the critical Reynolds number has been calculated to know the flow regime of the water flowing inside the coil. The Ito equation [28] (equation 6) has been used.

$$Re_{critical} = 20000\cdot\left(\frac{d_{int}}{D_H}\right)^{0.32} \quad \text{(eq. 6)}$$

According to the calculations, the water flows under laminar flow conditions (under the maximum mass flow that the thermostatic bath provides). Once the flow regime was determined, one of the correlations compiled in Naphon and Wongwises's review [29] was selected, namely, the correlation proposed by Xin and Ebadian [30] (equation 7). This allows the average interior forced convection coefficient in the completely developed region to be obtained.

$$Nu_{int} = (2.153 + 0.318\cdot De^{0.643})\cdot Pr^{0.177} \quad \text{(eq. 7)}$$

This correlation is valid in the ranges presented in equation 8:

$$20<De<2000; \quad 0.7<Pr<175; \quad 0.0267<d_{int}/D_H<0.0884 \quad \text{(eq.8)}$$

The properties of water were calculated at the average temperature of the water at the inlet and outlet, although they should be calculated at the film temperature, that is to say, at the average temperature between the coil wall temperature and the water temperature. The internal temperature of the coil is not known, so it would be necessary to turn to an iterative process for the solution of this problem, assuming this wall temperature [31]. Nevertheless,

given that the dominant resistance of the heat transfer process is found on the external side of the coil (convection in the stored water), the film temperature will not be very different from the average temperature between the inlet and outlet. Thus the different properties, and therefore the internal heat transfer coefficient, will not be significantly affected.

3.2.2 Analysis of the natural convective coefficient: comparison with correlations provided in the literature

The Nusselt number has been calculated from the natural convective coefficients obtained during the transient response of the tests, taking the external diameter of the coil as the characteristic length. Due to the low turn pitch, the coil can be considered as a horizontal tube. In addition, the Rayleigh number has been calculated from the thermal difference for each instant and the different thermophysical and rheological properties. These properties were calculated for a temperature defined according to equation 9 (the average between the HTF temperature and the water temperature):

$$T_{properties\ calculation} = T_{position\ 4} + \frac{\Delta T_m}{2} \quad \text{(eq. 9)}$$

In order to check the tests carried out with water, the calculated Nu_D-Ra_D values were compared to previous correlations provided by other authors who used the coil diameter as the characteristic length. Specifically, they have been compared to the correlations of Fernandez-Seara et al. [32] and Xin and Ebadian [33] and to the correlation for horizontal tubes given by Churchill and Chu [34]. Figure 10 shows this comparison. It can be observed that the experimental results follow the tendency of the correlations taken from the literature, although with a slightly lower slope. However, this could be due to the

greater uncertainty in the experimental results when working with the lowest values of the logarithmic mean temperature difference (corresponding to the lowest Rayleigh numbers).

3.2.3 Estimation of the heat losses from the tank to the ambient air

To estimate the energy stored by the TES system, firstly it is necessary to estimate the heat losses from the tank to the ambient air. For this purpose, a test was carried out in which the water contained in the tank was heated up to a temperature of 60ºC. Once 60ºC was reached, the water supply through the coil was stopped, and the water temperature evolution and the room temperature were recorded. From the energy balance on the tank (equation 10), a global heat loss coefficient was obtained:

$$\frac{dE_{water}}{dt} + \frac{dE_{insulation}}{dt} + \frac{dE_{stainless\ steel}}{dt} = \dot{m} \cdot c_p \cdot (T_{in} - T_{out}) - \dot{Q}_{amb} \quad \text{(eq. 10)}$$

Since the temperature evolution of the different elements of the tank is not known, and the storage capacity of these elements (insulation and stainless steel parts) is very low in comparison to the total heat capacity (lower than 5% when testing water as thermal storage material), only the energy stored by the water is taken into account to calculate this global heat loss coefficient. From equation 11, the coefficient U_{loss} can be obtained:

$$\dot{Q}_{amb} = U_{loss} \cdot A_{tank} \cdot (T_{water} - T_{amb}) \quad \text{(eq. 11)}$$

The values obtained were adjusted to a correlation type $U = c \cdot \Delta T^m$, obtaining the equation 12. This correlation was also used to estimate the heat losses from the tank containing the PCM emulsion, since the predominant resistance is the conduction in the insulation. The

320 average uncertainty estimated for this heat loss coefficient from the propagation error
321 formula is about 2%.

322 $U = 0.2456 \cdot \Delta T^{0.3471}$ (eq. 12)

323 **3.2.4 Energy stored by the TES system with water**

324 To calculate the energy stored by the tank, the energy balance on the system has been
325 obtained according to equation 13:

326 $E_{tank\ stored} = \int_i^e (\dot{Q}_{coil} - \dot{Q}_{amb}) \cdot dt$ (eq. 13)

327 In addition, the energy stored by the water has been calculated from the temperatures
328 recorded by the sensors that measure the interior temperatures of the water at different
329 heights. The energy stored by each one of the seven sections of the TES system has been
330 calculated from equation 14, considering that the whole section is found at the temperature
331 recorded by the corresponding sensor:

332 $E_{water\ stored} = m_{water} \cdot c_{p\ water} \cdot \Delta T_{water}$ (eq. 14)

333 It has been observed that when calculating the energy stored from the energy balance on the
334 system, the energy stored is higher than when calculating from the temperature evolution of
335 the water in the tank. The maximum difference observed in all the tests performed at the
336 end of the charging process was 12.5%. This result is reasonable, since in the calculation
337 from the energy balance on the system, the energy is that stored by the whole tank (that is
338 to say, water together with the insulation and the rest of the stainless steel components).
339 However, in the case of the calculation from the water temperature (energy balance on the

340 storage material), only the energy stored by the water is calculated. Furthermore, in this
341 case it is assumed that each section of the tank is found at the temperature that the sensor
342 records.

343 **3.3 Tests using a PCM emulsion as thermal storage material**

344 Firstly, the repeatability of the tests using the PCM emulsion was analyzed. Once the
345 repeatability was verified, the test series was started. As an example, figure 11 shows the
346 temperature evolution of the paraffinic emulsion at different heights of the tank, as well as
347 the HTF temperature at the inlet and outlet of the coil for a specific test. In this case, in
348 comparison to the water (figure 7), a larger temperature gradient along the central axis of
349 the tank is observed. As occurred with the water, the temperature recorded by the sensor in
350 position 7 was lower than for the other positions. These dead volumes mean that the
351 dynamic of the heat transfer is much slower, since the heat is mainly transfered by
352 conduction. Unlike the case of the tank containing water, it is observed that the temperature
353 measured by the sensor in position 1 is also lower. In the water case, although this section
354 was not taken up by part of the coil, the heat transfer by natural convection caused the
355 temperature of the section to increase.

356 In this case, when working with such a viscous PCM emulsion, the Rayleigh number is
357 within the range of 400-1000, compared to a Rayleigh number of around 10^6 for the tank
358 containing water. Consequently, the ratio of the heat transfer that takes place by convection
359 against that caused by conduction has decreased. In addition, it was observed in subsection
360 2.1.2 that the thermal conductivity of this paraffinic had decreased significantly in
361 comparison to water.

It is also observed that from around 7000 seconds, the dynamic of the system is limited by the low thermal gradient between the coil and the surrounding PCM and conditioned by the thermal diffusion to the dead volumes of the thermal energy transferred to the fluid. Thus, the resulting heat exchange between the coil and the TES fluid is lower than the sensitivity of the energy balance measurement. It is also observed that the paraffinic emulsion does not reach 50ºC, the HTF temperature. It reaches a temperature of 47.8ºC. A similar behavior is observed in the test results where the flow temperature was 60ºC. In this case, from 5000 seconds, the coil hardly transfers heat, but the temperature of the PCM emulsion in the central axis continues increasing. The behavior described here for the water and for the PCM emulsion was also observed by Huang et al. [12] in their slurry with a 50% PCM concentration.

3.3.1 Obtaining the global heat transfer coefficient. Comparison to the results with water.

When processing the data recorded in the study of the PCM emulsion or, to be more precise, when calculating the average thermal difference, it has been taken into account that in this case there is a temperature gradient in the PCM emulsion in the axial direction, so a priori a correction factor F=1 may not be used. This factor F provides the efficiency that a specific heat exchanger has in comparison to the efficiency of the heat exchanger that has the best thermal behavior, which is the counterflow heat exchanger. The factor F is calculated for a series of configurations and is generally represented graphically [35]. The tank with the helical coil could be considered as a one-shell-pass heat exchanger. For these tests, it has been observed that parameter F has values very close to 1 throughout the test time (between 0.97-1). For this reason the average thermal difference has been considered

as the mean logarithmic temperature difference with counter flows. Figure 12 shows the results obtained together with their uncertainty bands, in comparison to the results obtained for water. It can be seen that for the PCM emulsion the global heat transfer coefficient decreased from 500 W/(m^2·K) down to a value of around 100 W/(m^2·K). This reduction was expected due to the high viscosity of the PCM emulsion, reducing the heat transfer by convection. It is also observed that the U coefficient sharply decreases when the thermal difference decreases. If this global heat transfer coefficient is represented versus the temperature of the PCM emulsion in its central position in the tank, it can be seen that this value decreases abruptly once the temperature of the emulsion is around 45ºC (figure 13). This decrease in the U value from 45ºC, that is to say when the phase change ends, may be due to the abrupt increase in the viscosity observed in figure 5, giving rise to lower Rayleigh numbers. Furthermore, if the emulsion had a narrower phase change temperature range, the thermal difference in the heat exchanger would increase and the heat transfer would therefore improve.

3.3.2 Energy stored by the TES system with the PCM emulsion. Comparison with the water tank.

The same procedure as described in section 3.2.3 was followed for the TES system with the PCM emulsion. Figure 14 compares the results of the energy stored in some of the tests using the PCM emulsion and water as TES material, together with the uncertainty band. For the calculation of this error band, the maximum deviation obtained in the calibration process for each type of temperature probe was considered (±0.04°C for inlet and outlet water and ±0.15°C for TES fluid temperature measurement). The stored energy was calculated from the power curve, taking into account the heat losses of the tank (energy

408 balance on the system). If the energy stored for each TES system is compared at similar
409 average thermal energy temperatures, it can be seen that there is greater energy storage in
410 the TES systems with the low cost PCM emulsion, specifically 34% greater. However, due
411 to the non-ad hoc design of the tank for this material, the maximum energy that the material
412 could store is not reached within a practical response time period for this application,
413 showing system efficiencies of about 75%. This problem, although less significant, also
414 occurs with the water tanks, with efficiencies of about 90%.

415 The energy stored was also calculated from the temperatures recorded in the axial direction
416 of the tank and from the enthalpy-temperature curve obtained with the DSC (energy
417 balance on the storage material). For these calculations, it has been considered that each
418 section was found completely at the temperature recorded by the sensor. The average
419 temperature was weighted, based on the mass of each section. Figure 15 shows a
420 comparison of the energy stored together with its uncertainty band, according to the
421 calculation methodology. In the case of the thermal energy variation of the TES fluid, the
422 corresponding uncertainty of the DSC measurements was considered (5%) which results in
423 a greater contribution to this error, since the temperature increment –compared to the
424 accuracy of the probes- is rather high. It is observed that for the tests carried out with a flow
425 temperature of 50ºC, the energy stored calculated by the energy balance on the system is
426 11.4% lower than that calculated by the energy balance on the storage material, probably
427 due to the low temperature decrease of the water flowing in the coil during the experiment.

428 **4. Comparison to other TES systems**

The ultimate purpose of this work is the comparison of TES systems using PCM emulsions with traditional TES systems using water, and with systems where the PCM is macroencapsulated or in bulk form, confined in the tank, using water as HTF in the heat exchange. For this reason, the results obtained in this work have been compared to other systems studied in the literature, whose main characteristics are compiled in table 1. The choice of TES systems taken from the literature for this comparison was determined by the requirement to consider different encapsulated geometries and by the use of a paraffin as a PCM, since the emulsion is of a paraffinic nature. If TES systems with salt hydrates had been considered, the comparison with TES systems with PCM slurries would not have been entirely appropriate given the higher values of phase change enthalpy and thermal conductivity of these inorganic PCMs. In addition, these systems are at a less advanced stage of development level due to problems of corrosion, phase segregation and subcooling. The phase change temperature range of the systems considered in this comparison is not of interest, since the thermophysical properties are independent. Other TES systems with PCM slurries have also been taken into account. Ice systems, which provide the highest energy density values and higher thermal conductivity values, have also been included in the comparison.

To try to establish as rigorous a comparison as possible from the data presented in the works compiled in table 1, three parameters have been compared: the energy density of the system, their global heat transfer coefficient (U) and the relation between the heat transfer area and the tank volume (A/V).

Some of the results compiled here have been taken from a work by Mazo et al. [36] in which the U value was calculated from experimental data presented in previously published

452 articles using either the logarithmic mean temperature difference or the ε-NTU
453 methodology. The TES systems examined in the present work have also been chosen owing
454 to the amount of data available about them in the literature and to their easier treatment.

455 In some cases only the energy density of the storage material has been shown, and not the
456 energy density associated to the whole TES system, due to the lack of data in the articles
457 found in the literature. The ideal solution would be to calculate the energy density of the
458 system, calculated from the energy balance executed on the system, taking into account its
459 capacity efficiency, that is to say, the material fraction that has undergone phase change.

460 In order to be able to plot a 2D graphic from the values of these three parameters, the global
461 heat transfer coefficient, the heat transfer area and the tank volume ratio have been grouped
462 together as a single parameter. This new parameter, (U·A/V), may provide some notion of
463 the thermal power of the system in relation to its volume. It is also useful because it allows
464 systems of very different scales to be compared whenever such systems are similar in terms
465 of heat transfer.

466 Figure 16 shows a graphic representation of the results of the comparison. It is observed
467 that the TES systems c) and d) described by Medrano et al. [37] have the best thermal
468 response but the worst energy density due to their low content capacity of PCM. The TES
469 systems with a larger storage capacity are those described by Chen et al. [40] and
470 Bédécarrats et al. [41]. It must be kept in mind that these two systems use ice as PCM,
471 which has a significantly higher phase change enthalpy: 333 kJ/kg. If a paraffin had been
472 used instead of ice, this storage capacity would have been reduced at least down to values
473 similar to those of the systems described by Torregrosa-Jaime et al. [38] and López-

Navarro et al. [39], or to the PCM slurry systems with high PCM concentrations. Torregrosa-Jaime et al. [38] first analyzed experimentally a commercial ice storage tank around 18 spiral-shaped coils, but containing the paraffin RT8. The energy density of the system could have been larger, if dead volumes in the base and center had been avoided, which represented 31%. Subsequently, López-Navarro et al. [39] designed their own prototype based on this recent experiment. With their new design, they achieved 78% of the maximum capacity.

It can be seen in table 1 that although the TES systems with PCM slurry are not competitive against the sensible systems with water in terms of their global heat transfer coefficient, they do show significant improvements over traditional latent systems. However, these systems have a lower A/V ratio, which makes the parameter (U·A/V) equal. These PCM slurry systems have a higher energy density than the water systems, but slightly lower than some of the conventional latent systems [38-41].

The system analyzed in the present study has a worse thermal response due to the high viscosity of the sample and to the wide phase change temperature range. The improvement in terms of the energy density of the system was not as great as expected because of the non-specific design of the tank resulting in dead volumes which did not undergo complete melting during a time period practical for an engineering application. In spite of this, the improvement in the energy density as compared to water systems renders this system with PCM emulsion promising as a thermal storage system. However, different measures could be adopted to improve its response, as for instance:

- A specific design of the tank to avoid dead volumes and thus improve the energy density

- Increasing the U·A/V parameter. This could be enhanced in different ways:

1) Increasing the heat transfer area, not involving a considerable reduction in the storage capacity of the system;

2) Improving the global heat transfer coefficient by developing PCM emulsions with a lower viscosity and a narrower phase change temperature range, which would raise the product price, or by considering TES systems such as those described by Vorbeck et al. [43] and Kappels et al. [44], using a cylindrical tank and a plate heat exchanger external to the tank. This latter suggestion would increase the heat transfer area and the global heat transfer coefficient when pumping the PCM slurry through the heat exchanger.

The possibility of including stirrers in the tank has also been contemplated. These stirrers would initiate the motion of the emulsion inside the tank, boosting the convection. On the other hand, due to the higher shear rates induced by the stirrers and experienced by the PCM emulsion, the emulsion viscosity would decrease. The electrical consumption as well as the volume that the stirrers would take up would also have to be analyzed.

5. Conclusions

A low cost PCM emulsion has been characterized. Both its thermophysical and rheological properties have been determined and compared to the properties of water. The PCM emulsion improved the TES capacity per mass of around 50% compared to water in the temperature range of 30-55ºC. The thermal diffusivity measured in the monophase states of the dispersed paraffin decreased significantly, by about 40%. The variation of the density values with temperature was higher than for water, that is to say its volumetric expansion

coefficient was higher. This enhancement would promote the heat transfer by convection in tanks containing this PCM emulsion. A flow curve has been obtained in relation to the rheological characterization showing an abrupt increase in the viscosity compared to water (from 2 to 5 orders of magnitude depending on the shear rate). This caused an opposite effect on the convection heat transfer phenomenon.

A conventional TES tank has been analyzed, containing on the one hand the paraffinic emulsion and on the other hand water, in order to compare the heat transfer process and the energy stored by each of these two systems. As a consequence of the increase in the viscosity when working with the PCM emulsion, a significant decrease in the global heat transfer coefficient was observed, from 500 down to 100 ($W/(m^2 \cdot K)$). This considerably increased the charging time of the tank.

The energy storage density calculated from the energy balance on the tank was 34% higher in the case of the tank filled with the PCM emulsion than for the tank with water for a similar temperature of the storage fluid. The energy storage density could be improved with a specific design of the tank, avoiding dead volumes.

Both TES systems have been compared to other TES systems with PCM analyzed in the literature. This was based on a comparison of the global heat transfer coefficient, of the heat transfer area vs. the tank volume ratio and of the storage energy density. The comparison has shown that the system with the PCM emulsion represents a promising solution as a thermal storage system.

As regards future work, it would be of interest to be able to record the temperatures of the PCM emulsion at different radiuses, not just in the central axis of the tank. By recording

temperatures in zones closer to the coil, it would be possible to analyze the heat transfer in the radial direction and also to analyze more rigorously the heat transfer by conduction and convection.

It would also be of interest to systematize the comparison of the results here presented with those obtained by other researchers who have studied these new types of TES systems. Such a comparison may be accomplished following an analysis of the thermophysical and rheological characteristics of the slurries and of the final results in terms of the heat transfer and energy density of the TES systems.

Acknowledgements

The authors would like to thank the Spanish Government for partially funding this work within the framework of research projects (MICINN-FEDER): ENE2011-28269-C03-01 and ENE2014-57262-R. Mónica Delgado is also grateful to the Fundación Iberdrola for financial support for this research project under the call "Ayudas a la Investigación en Energía y Medio Ambiente. Convocatoria 2013". The authors would like to acknowledge the companies Lapesa S.A. and RLESA-Repsol for their collaboration in this research. Authors would like to acknowledge the use of Servicio General de Apoyo a la Investigación-SAI, Universidad de Zaragoza.

References

[1] Chen L, Wang T, Zhao Y, Zhang X. Characterization of thermal and hydrodynamic properties for microencapsulated phase change slurry (MPCS). Energy Convers Manage 2014;79:317-33.

[2] Zhang P, Ma ZW, Wang RZ. An overview of phase change material slurries: MPCS and CHS. Renew Sust Energy Rev 2010;14(2):598-614.

563 [3] Delgado M, Lázaro A, Mazo J, Zalba B. Review on phase change material emulsions
564 and microencapsulated phase change material slurries: Materials, heat transfer studies and
565 applications. Renew Sust Energy Rev 2012;16(1):253-73.
566 [4] Youssef Z, Delahaye A, Huang L, Trinquet F, Fournaison L, Pollerberg C et al. State of
567 the art on phase change material slurries. Energy Convers Manage 2013;65:120-32.
568 [5] BASF Micronal http://www.micronal.de/portal/basf/ien/dt.jsp?setCursor=1_290798
569 (last access May 2015)
570 [6] Aero http://www.aero.si/ps/prg_microenc.htm (last access May 2015)
571 [7] Fraunhofer ISE http://www.ise.fraunhofer.de/en/business-areas/storage-
572 technologies/research-topics/latent-heat-storage/latent-heat-storage (last access May 2015)
573 [8] Fraunhofer UMSICHT http://www.umsicht.fraunhofer.de/en/press-
574 media/2014/crysolplus-pcs-energy-storage.html (last access May 2015)
575 [9] Royon L, Guiffant G. Forced convection heat transfer with slurry of phase change
576 material in circular ducts: A phenomenological approach. Energy Convers Manage
577 2008;49(5):928-32.
578 [10] Heinz A, Streicher W. Application of phase change materials and PCM-slurries for
579 thermal energy storage, Ecostock Conference, New Jersey (USA) 2006.
580 [11] Diaconu BM, Varga S, Oliveira AC. Experimental study of natural convection heat
581 transfer in a microencapsulated phase change material slurry. Energy 2010;35(6):2688-93.
582 [12] Huang MJ, Eames PC, McCormack S, Griffiths P, Hewitt NJ. Microencapsulated
583 phase change slurries for thermal energy storage in a residential solar energy system.
584 Renew Energy 2011;26(11):2932-39.
585 [13] Jegadheeswaran S, Pohekar SD. Performance enhancement in latent heat thermal
586 storage system: A review. Renew Sust Energy Rev 2009;13(9):2225-44.

587 [14] Kosny J, Shukla N, Fallahi A. Cost analysis of simple phase change material-
588 Enhanced building envelopes in Southern U.S., U.S. Department of Energy. January 2013.
589 [15] Peñalosa C, Lázaro A, Delgado M, Dolado P, Zalba B. Valorization of paraffin as low
590 cost phase change material. Characterization for using in thermal energy storage,
591 Eurotherm Seminar #99: Advances in Thermal Energy Storage, Lleida (Spain), 28-30 May
592 2014.
593 [16] Biswas K, Abhari R. Low-cost phase change material as an energy storage medium in
594 building envelopes: Experimental and numerical analyses. Energy Convers Manage
595 2014;88:1020-31. 88
596 [17] Dolado P. Almacenamiento térmico de energía mediante cambio de fase. Diseño y
597 modelización de equipos de almacenamiento para intercambio de calor con aire. Ph.D.
598 Thesis. University of Zaragoza, 2011.
599 [18] Royon L, Perrot P, Guiffant G, Fraoua S. Physical properties and thermorheological
600 behaviour of a dispersion having cold latent heat-storage material. Energy Convers Manage
601 1998;39(15):1529-35.
602 [19] Lázaro A. Thermal Energy Storage with Phase Change Materials. Building
603 applications: Material behavior characterization and experimental setup for testing air-PCM
604 heat exchangers. Ph.D. Thesis. University of Zaragoza, 2008.
605 [20] Zhang Y, Jiang Y, Jiang Y. A simple method, the T-history method, of determining
606 the heat of fusion, specific heat and thermal conductivity of phase-change materials. Meas
607 Sci Technol 1999;10(3):201-5.
608 [21] Lázaro A, Günther E, Mehling H, Hiebler S, Marín JM, Zalba B. Verification of a T-
609 history installation to measure enthalpy versus temperature curves of phase change
610 materials. Meas Sci Technol 2006;17(8):2168-74.

611 [22] Lázaro A, Peñalosa C, Solé A, Diarce G, Haussmann T, Fois M et al. Intercomparative
612 tests on phase change materials characterisation with differential scanning calorimeter.
613 Appl Energy 2013;109:415-20.
614 [23] Gschwander S, Haussmann T, Hagelstein G, Sole A, Cabeza LF, Diarce G et al.
615 Standardization of PCM characterization via DSC. The 13th International Conference on
616 Energy Storage. Greenstock 2015, Beijing (China), 19-21 May 2015.
617 [24] Delgado M, Lázaro A, Peñalosa C, Zalba B. Experimental analysis of the influence of
618 microcapsule mass fraction on the thermal and rheological behavior of a PCM slurry. Appl
619 Therm Eng 2014;63(1-5):11-22.
620 [25] Delgado M. Analysis of microencapsulated phase change material slurries and phase
621 change material emulsions as heat transfer fluid and thermal storage material. Ph.D. Thesis.
622 University of Zaragoza, 2013.
623 [26] ASTM G1-03 (2011) Standard Practice for Preparing, Cleaning, and Evaluating
624 Corrosion Test Specimens.
625 [27] Delgado M, Lázaro A, Mazo J, Marín JM, Zalba B. Experimental analysis of a
626 microencapsulated PCM slurry as thermal storage system and as heat transfer fluid in
627 laminar flow, Appl Therm Eng 2012;36:370-7.
628 [28] Ito H. Friction factor for turbulent flow in curved tube. J Basic Eng-T ASME
629 1959;81:123-34.
630 [29] Naphon P, Wongwises S. A review of flow and heat transfer characteristics in curved
631 tubes. Renew Sust Energy Rev 2006;10(5)463-90.
632 [30] Xin RC, Ebadian MA. The effects of Prandtl numbers on local and average convective
633 heat transfer characteristics in helical pipes. J Heat Trans-T ASME 1997;119(3):467-73.

634 [31] Prabhanjan DG, Rennie TJ, VijayaRaghavan GS. Natural convection heat transfer
635 from helical coiled tubes. Int J Therm Sci 2004;43:359-65.
636 [32] Fernández-Seara J, Diz R, Uhía FJ, Sieres J, Dopazo JA. Thermal analysis of a
637 helically coiled tube in a domestic hot water storage tank.Proceeding of the 5th International
638 Conference on Heat Transfer, Fluid Mechanics and Thermodynamics. Sun City, South
639 Africa, 2007.
640 [33] Xin RC, Ebadian MA. Natural convection heat transfer from helicoidal pipes. J
641 Thermophys Heat Tr 10 (2) (1996), pp. 297-302.
642 [34] Churchill SW, Chu HHS. Correlating equations for laminar and turbulent free
643 convection from a horizontal cylinder. Int J Heat Mass Tran 1975;18:1049-53.
644 [35] Incropera FP, Dewitt DP, Bergman TL, Lavine AS. Fundamentals of Heat and Mass
645 Transfer. Wiley, New York, 1996.
646 [36] Mazo J, Delgado M, Dolado P, Lázaro A, Peñalosa C, Marín JM et al.
647 Almacenamiento térmico de energía con materiales de cambio de fase en aplicaciones de
648 refrigeración. Avances en Ciencias y Tecnologías del Frio VII. VII Congreso Ibérico de
649 Ciencias y Tecnologías del Frio, Tarragona (Spain), 18-20 June 2014.
650 [37] Medrano M, Yilmaz MO, Nogués M, Martorell I, Roca J, Cabeza LF. Experimental
651 evaluation of commercial heat exchangers for use as PCM thermal storage systems. Appl
652 Energy 2009;86(10):2047-55.
653 [38] Torregrosa-Jaime B, López-Navarro A, Corberán JM, Esteban-Matías JC, Klinkner L,
654 Payá J. Experimental analysis of a paraffin-based cold storage tank. Int J Refrig
655 2013;36(6):1632-40.
656 [39] López-Navarro A, Biosca-Taronger J, Corberán JM, Peñalosa C, Lázaro A, Dolado P
657 et al. Performance characterization of a PCM storage tank. Appl Energy 2014;119:151-62.

[40] Chen S, Chen C, Tin C, Lee T, Ke M. An experimental investigation of cold storage in an encapsulated thermal storage tank. Exp Therm Fluid Sci 2000;23(3-4):133-44.

[41] Bédécarrats JP, Strub F, Falcon B, Dumas JP. Phase-change thermal energy storage using spherical capsules: performance of a test plant. Int J Refrig 1996;19(3):187-96.

[42] Streicher W, Heinz A, Puschnig P, Schranzhofer H, Eisl G, Heimrath R et al. Fortschrittliche Wärmespeicher zur Erhöhung von solarem Deckungsgrad und Kesselnutzungsgrad sowie Emissionsverringerung durch verringertes Takten. Projekt zum IEA-SHC Task 32, 2006.

[43] Vorbeck L, Gschwander S, Thiel P, Lüdemann B, Schossig P. Pilot application of phase change slurry in a 5 m^3 storage. Appl Energy 2013;109:538-43.

[44] Kappels T, Kohnen T, Hanu LG, Pollerberg C. Design and retroffiting of a cold storage replacing water with phase change slurries. Eurotherm Seminar #99. Advances in Thermal Energy Storage. Lérida (Spain), 28-30 May 2014.

Figure captions

Figure 1. Enthalpy-temperature curves for the low cost PCM emulsion compared to water.

Figure 2. Thermal diffusivity values for the PCM emulsion in comparison to water. Test conditions: Voltage=1538V; Gain=127; Filter transmission=100%.

Figure 3. Density-temperature values for the PCM emulsion in comparison to water.

Figure 4. Viscosity-shear rate curves for the PCM emulsion at 25ºC compared to water.

Figure 5. Viscosity-temperature curves at a heating and cooling rate of 0.5 K/min. Shear rate=100 s^{-1}.

Figure 6. Position of temperature sensors along the central axis of the tank.

680 **Figure 7.** Temperature evolution of the HTF at the inlet and outlet of the coil and
681 temperature evolution of the water inside the tank along the central axis. Flow
682 temperature=50ºC; Mass flow=420 kg/h.
683 **Figure 8.** Global heat transfer coefficient for different tests together with the uncertainty
684 band.
685 **Figure 9.** Relationship between the global heat transfer coefficient, the average temperature
686 difference and the HTF temperature decrease.
687 **Figure 10.** Experimental Nu-Ra values for the water tank in comparison to the literature
688 correlations. Coil tube diameter as characteristic length.
689 **Figure 11.** Temperature evolution of the HTF at the inlet and outlet of the coil and
690 temperature evolution of the PCM emulsion inside the tank along the central axis. Flow
691 temperature=50ºC; Mass flow=420 kg/h.
692 **Figure 12.** Global heat transfer coefficient for the PCM emulsion in comparison to water,
693 together with the uncertainty band.
694 **Figure 13.** Global heat transfer coefficient of the PCM emulsion together with the
695 uncertainty band, depending on its temperature.
696 **Figure 14.** Thermal energy stored by the tank containing the PCM emulsion and by the
697 tank containing water for different tests.
698 **Figure 15.** Thermal energy stored by the system and by the fluid storage for different tests
699 with the PCM emulsion.
700 **Figure 16.** TES systems comparison in terms of energy density and heat transfer rate.
701 **Table captions**
702 **Table 1.** Characteristics of the different TES systems with which the tank containing the
703 PCM emulsion and water has been compared.

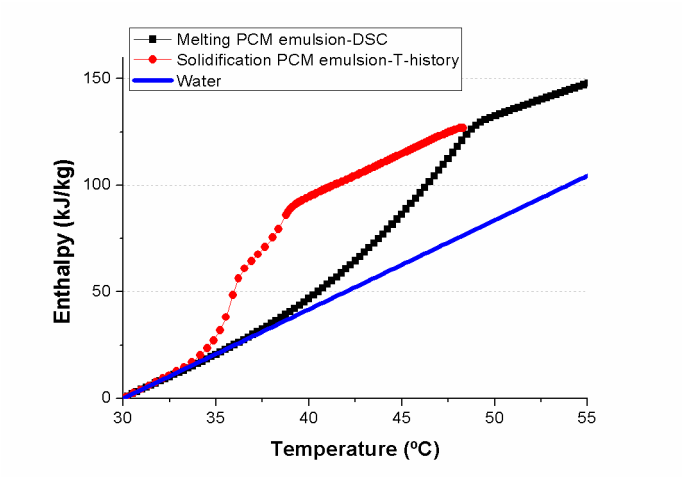

704

705 Figure 1.

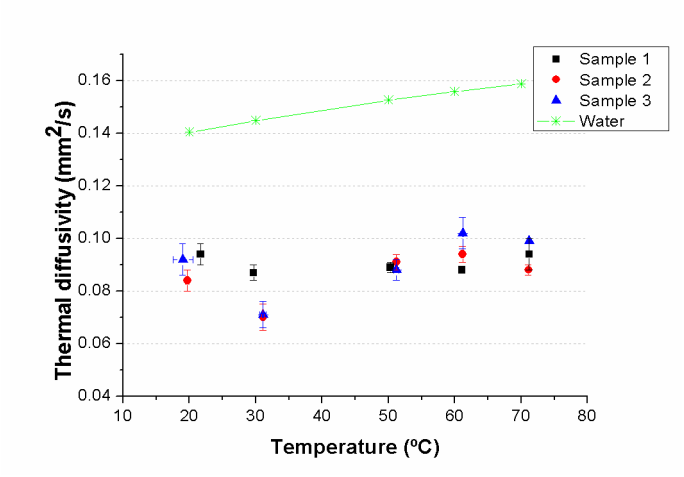

706

707 Figure 2.

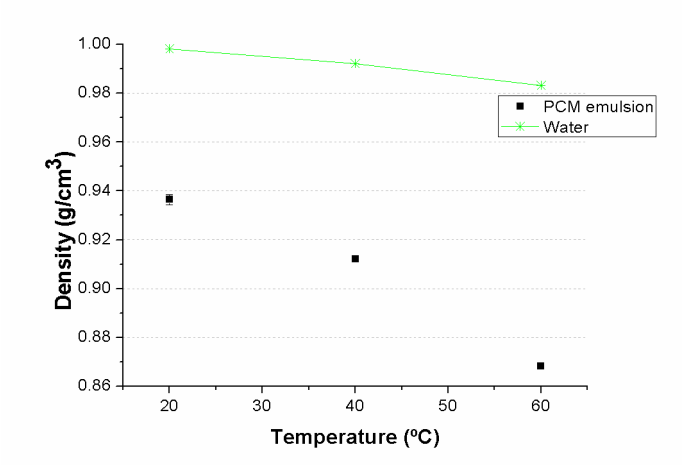

708

709 Figure 3.

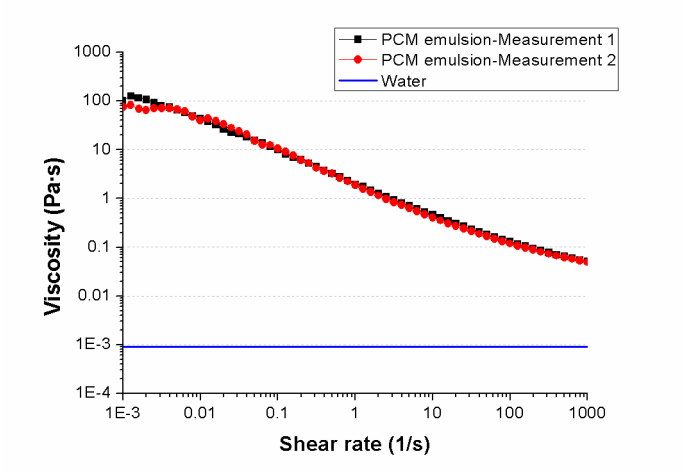

710

711 Figure 4.

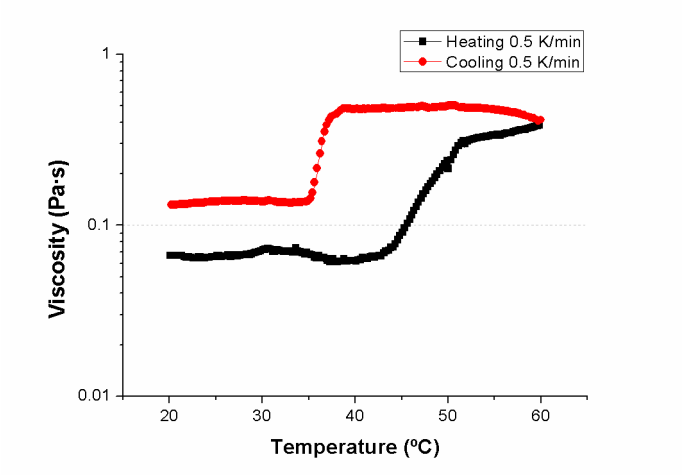

712

713 Figure 5.

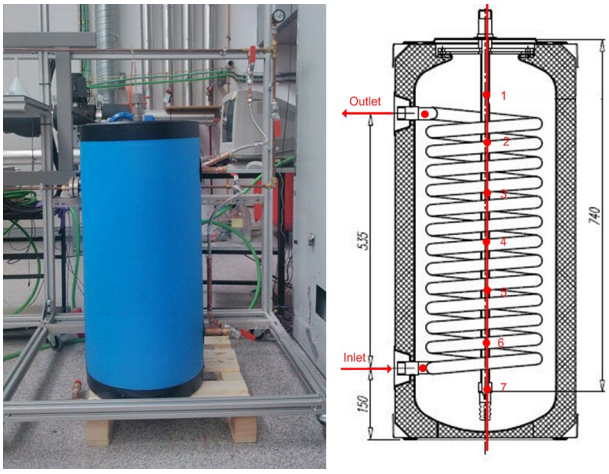

714

715 Figure 6.

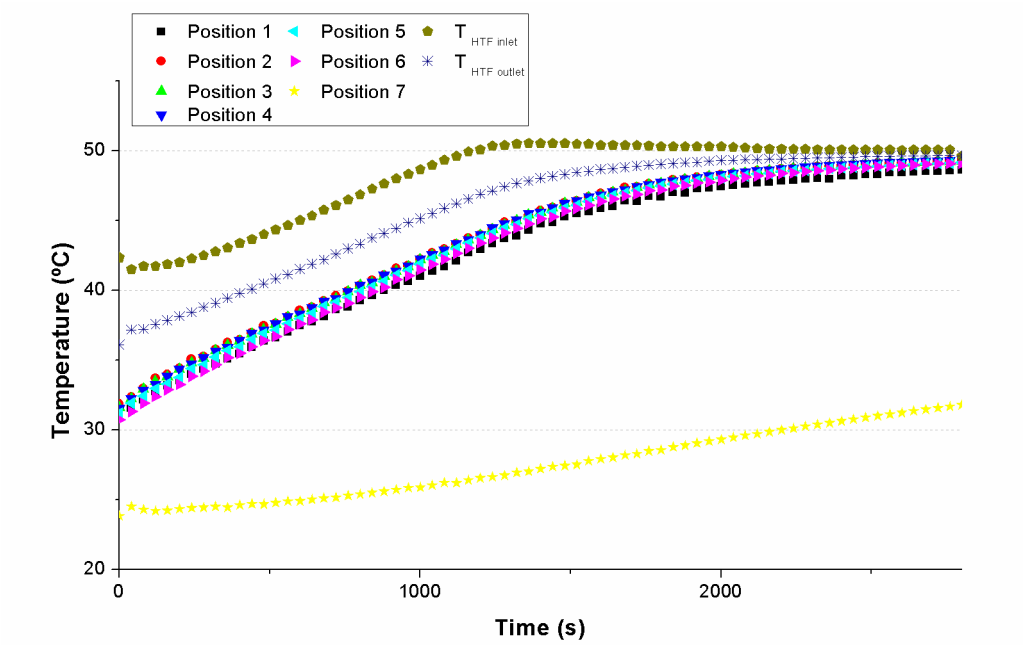

716

717 Figure 7.

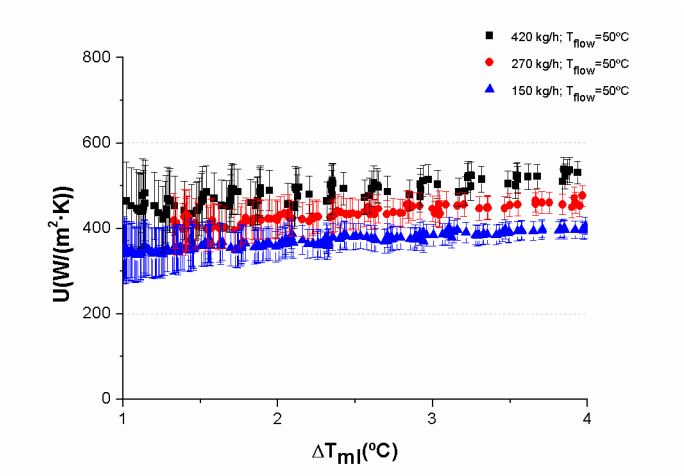

718

719 Figure 8.

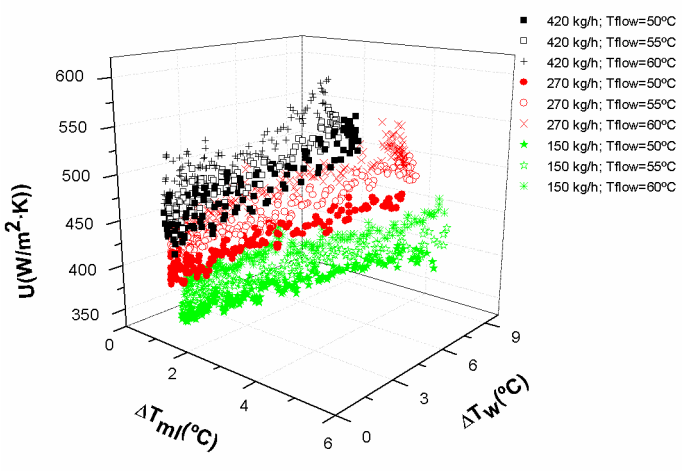

720

721 Figure 9.

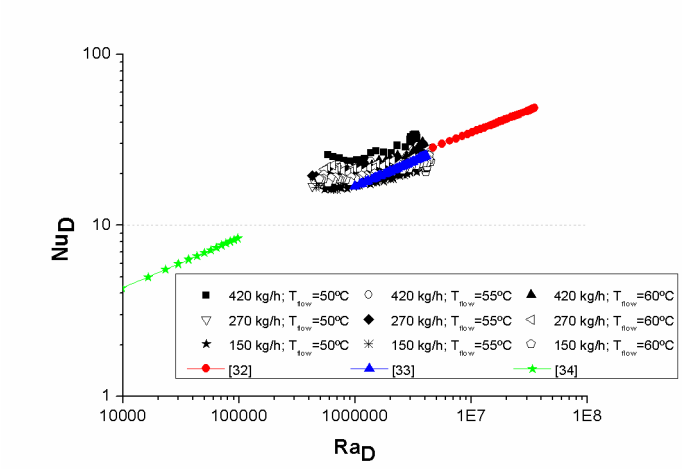

722

723 Figure 10.

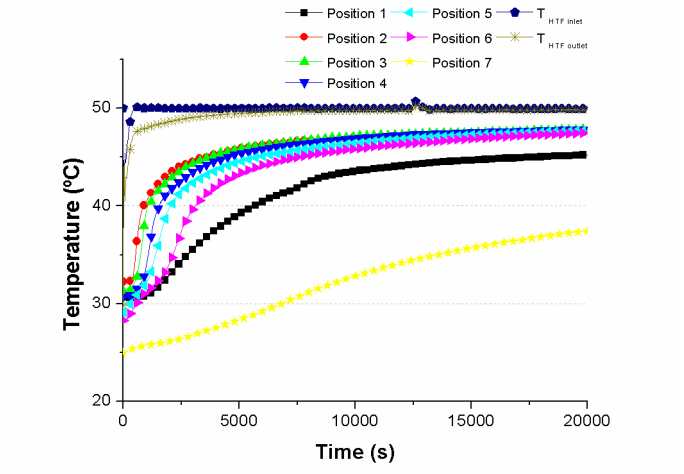

724

725 Figure 11.

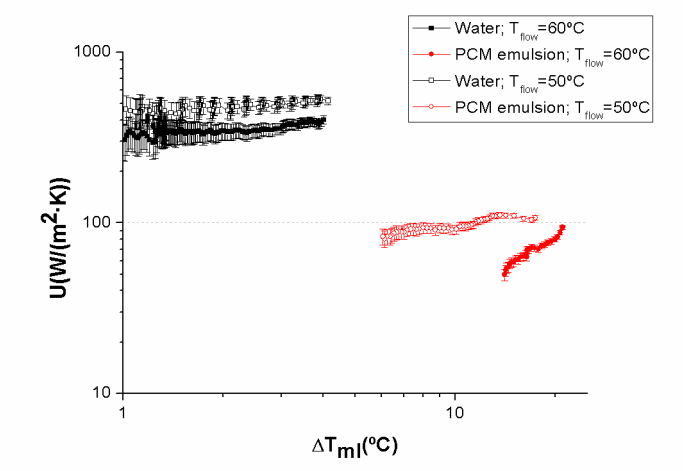

726

727 Figure 12.

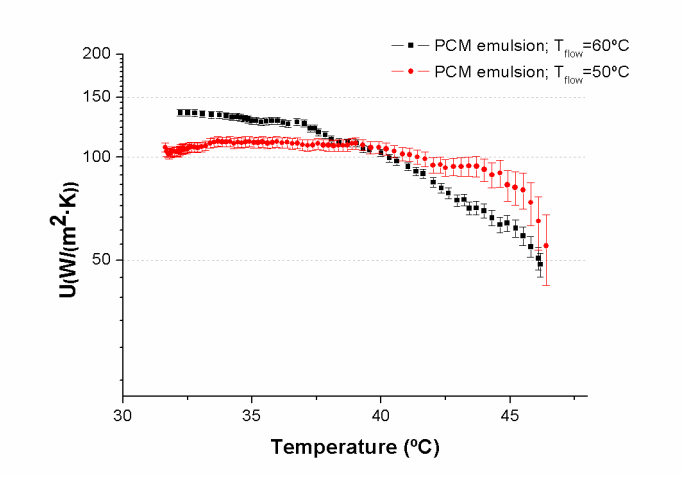

728

729 Figure 13.

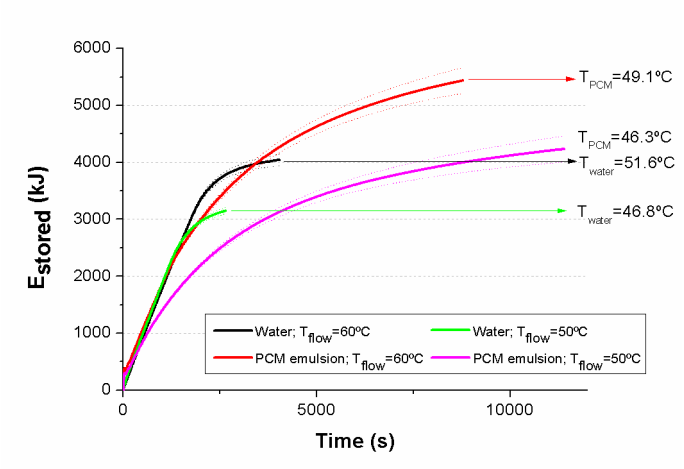

730

731 Figure 14.

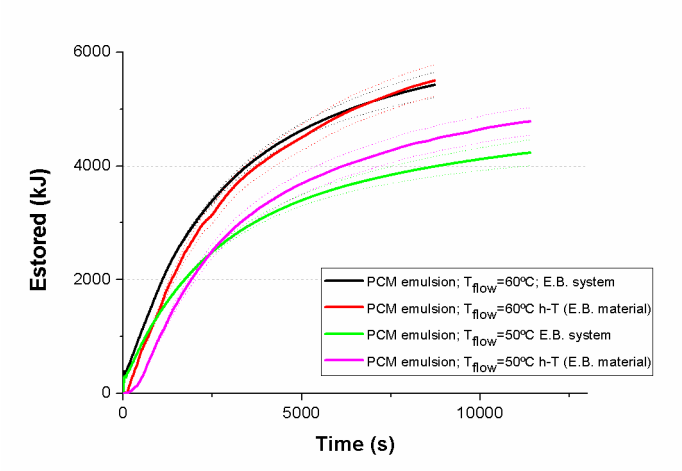

732

733 Figure 15.

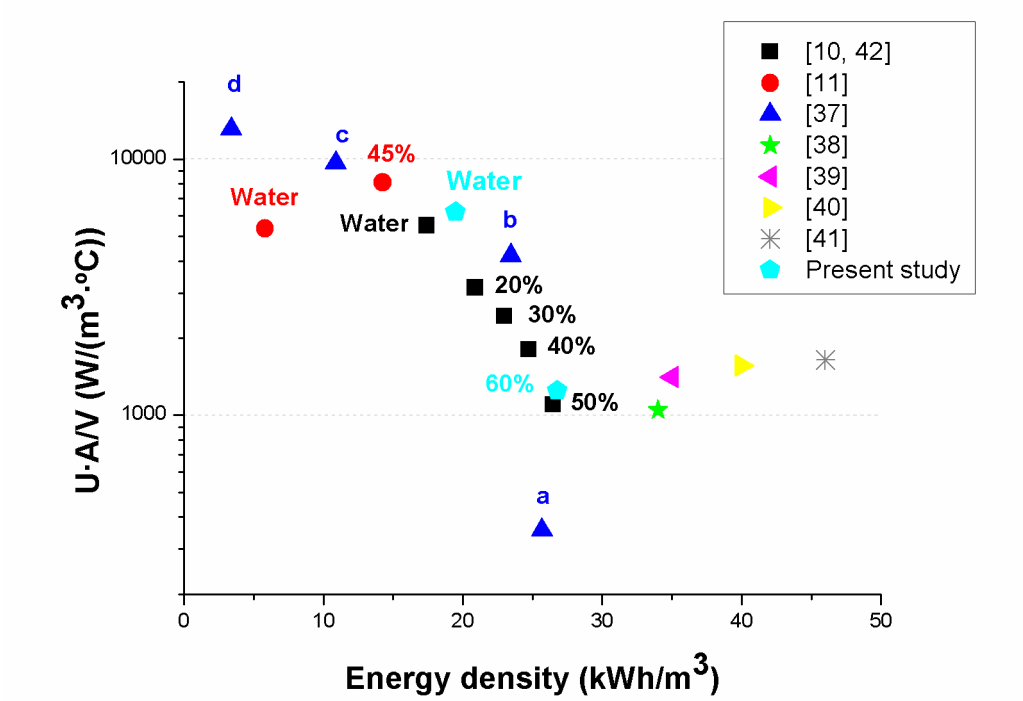

734

735 Figure 16.

736

737

738

739

740

Ref	Type of encapsulation	Heat storage material	E [kWh/m^3]	U [W/(m^2·K)]	A/V [m^{-1}]	Comments
[37]	a) Double pipe heat exchanger in the annular space	RT35	25.67	30*	11.83	*Approximate U values taken from graphs (melting case)
	b) Same as 1, but with external fins on the copper tube		23.44	60*	69.89	
	c) Compact heat exchanger, with PCM between coil and fins		10.89	50*	193.18	
	d) Plate and frame heat exchagner, with PCM in half of the passages		3.39	15*	875.00	
[38]	Bulk PCM inside Calmac Icebank 1098C	RT8	34.00	35	30.00	
[39]	Bulk PCM inside a tank (prototype)	RT8	35.00	64	22.00	
[40]	Cylindrical capsules (diameter: 7.3 cm; length: 24 cm)	Ice	40.00	65	24.00	
[41]	Spherical capsules (diameter: 7.7 cm)	Ice	46.00	35	47,00	
[10, 42]	Tank with a helical coil inside	a) 20% PCM slurry	20.90*	400**	7.85	*Energy density taken from h-T curves. Temperatures range 30-65ºC. Energy density having considered only the heat stored by the material and its volume . **Natural convection coefficient instead of the global heat transfer coefficient. This should be slighly smaller.
		b) 30% PCM slurry	22.99*	310**	7.85	
		c) 40% PCM slurry	24.73*	230**	7.85	
		d) 50% PCM slurry	26.47*	140**	7.85	
		e) Water (sensible)	17.42*	700**	7.85	
[11]	Tank with a helical coil inside	a) 45% PCM slurry	16.37*	1086**	7.47	*Energy density taken from h-T curves obtained from DSC. Temperature range 2-7ºC. Energy density having considered only the heat stored by the material and its volume . **Natural convection coefficient instead of the global heat transfer coefficient. This should be slighly smaller.
		b) Water (sensible)	5.81*	717**	7.47	

741 Table 1.